A Multiband Polarisation-Insensitive Microwave Metamaterial Absorber Comprising of Concentric Open and Closed Loop Resonators

Subbarao Genikala[1, 2*], Anumoy Ghosh[1], and Bappadittya Roy[3]

[1]Department of Electronics and Communication Engineering, NIT Mizoram, Aizawl, India

[2]Department of Electronics and Communication Engineering, Madanapalle Institute of Technology & Science (MITS) Deemed to be University, Madanapalle, India

[3]School of Electronic Engineering, VIT-AP University, Beside AP Secretariat, Amaravati, 522241, Andhra Pradesh, India

Corresponding author: Subbarao Genikala (e-mail: subbarao.genikala@gmail.com).

ABSTRACT An ultra-thin polarization-insensitive triple-band microwave metamaterial absorber is designed and reported in this paper. It comprises of multiple concentric metallic resonators on a metal backed substrate. The outermost resonator is a split structure whereas the inner resonators are closed loops with protruding arms. The overall structure has four-fold symmetry and compact size. It exhibits near unity three absorption peaks at 3.46 GHz, 4.98 GHz, and 7.26 GHz, respectively with exactly same response for all the polarization angles, thereby attaining polarization-insensitive behaviour. The structure demonstrates good stability under oblique incidence up to 60^{o} incident angle for both transverse electric (TE) and transverse magnetic (TM) modes of propagation. The shielding effectiveness (SE) at all three peaks is beyond 35 dB. An equivalent circuit is proposed for the designed structure. The absorption mechanism is elaborated using electric (E) and magnetic (H) field analysis. An array of 26 × 26 unit cells of the proposed structure is fabricated and the measured results closely resemble the simulated results. The proposed structure is compared with recent literature to highlight its advantage in terms of wider angular stability under oblique incidence polarization insensitivity, compactness and shielding effectiveness.

INDEX TERMS Electromagnetic interference (EMI), Microwave metamaterial absorbers, Polarisation insensitive, shielding effectiveness (SE).

1. INTRODUCTION

ELETROMAGNETIC absorbers are very carefully developed structures that absorb a particular range of frequencies in the incident electromagnetic spectrum to minimize radar cross-section. With advancements in interference and detection technology, it's crucial to develop efficient shielding and absorption technologies for stealth applications and electromagnetic compatibility. Metamaterial absorbers are metal structures that filter out the transmission and reflection of electromagnetic waves. The perfect metamaterial absorber (PMA) design construction creates resonance at precise frequencies and converts the incoming electromagnetic wave into different kinds of energy. It is based on the unit cell resonant behavior to achieve perfect absorption. The metamaterial (MM) absorbers are typically made by adjusting their effective permittivity and permeability to coincide with the free space impedance. This allows the electromagnetic (EM) signal to penetrate completely into the absorber alongside the EM radiation, which ohmic and dielectric losses can scatter.

Materials used for absorbers are designed to reduce the electromagnetic wave reflection in the microwave frequency range. Microwave metamaterial absorbers are utilized for a range of applications, including electronic warfare and aerospace defense, to reduce electromagnetic interference and improve signal integrity. Metamaterials provide unparalleled control over electromagnetic waves, including polarization insensitivity along with tunable absorption bands. These materials led to absorbers with broad bandwidth and reduced weight, suitable for use in military stealth technology and consumer electronics. The cooperation is expected to bring new achievements in the fields of communication, sensing, optical applications [1] and electromagnetic interference mitigation. The field of microwave absorbers has made significant progress in recent years, and the present researchers are aiming to create dual band absorbers and multi band absorbers, which are compact, light, and capable of absorbing microwave signals over a broad spectrum of frequencies. With the invention of metamaterial absorber development, many of the practical limitations of traditional absorbers were overcome. The literature has numerous reports on single-band as well as multi-band absorbers for applications in microwaves.

A small folded square structure has been designed for dual-band unpolarized microwave application, especially for C band and Ku band applications [2]. Likewise, ultra-thin dual band perfect microwave metamaterial absorbers for microwave applications were proposed [3] highlighting the compact and versatile designs of microwave absorbers. Multi Polarization-insensitive microwave metamaterial absorbers that are based on band polarization-insensitive meta surface [4-7] have been picked up because of their characteristic ability to absorb at multiple frequency bands without any polarization influence. This method employs square and circular loops [8-9] and lumped elements for multi band or broadband absorption properties. The frequency coverage is further extended by tri-band microwave perfect metamaterial absorbers [10-12] which demonstrate the development toward absorbers that exhibit multiple absorption peaks [13]. To achieve a compact and efficient design [14-15] researchers have looked into the design of an ultra-thin and compact triple-band, polarization-sensitive microwave metamaterial absorber [16, 17]. The absorbers show polarization sensitivity with triple-band absorption characteristics suitable for various satellite and Wi-fi applications [18-19]. The development of electromagnetic wave absorbers with the use of negative refractive index materials has also been a major development that has utilized novel materials in the design of absorbers [20]. Additionally, double-layer structures [21], have been designed for dual-band metamaterial absorbers, particularly focusing on stealth and biomedical applications [22-23], and radar cross-section reduction [24]. In particular, electromagnetic metamaterial absorbers are a novel application, demonstrating the potential of absorbers in sensing and detection technologies [25]. A number of optimization methods have been developed, including neural network algorithms [26]. They were used for the design of multi-band absorbers of better performance. The polarization-insensitive EM absorbers applications include electromagnetic compatibility/ electromagnetic interference (EMC/EMI) have also been developed as a result of the design considerations [27-29]. Further innovations consist of triple-band ultrathin conformal metamaterial absorbers [30] and [31-32] which provide wideband absorption in C-band and X frequency bands. Materials have been developed, such as ZnSe [33] that have allowed the realization of triple band absorbers. They have also proposed triple-band perfect metamaterial absorbers that are polarization-insensitive and well suited for terahertz sensing [34]. Further, single, double and triple band microwave absorbing materials demonstrate versatility in a range of frequencies. More recently, triple-band square-interlinked-rhombus shaped metamaterial absorbers are developed, which can be used for microwave C and X-band applications with improved performance [35]. These absorbers are on-going attempts to improve the absorption properties while still keeping the device compact and light. Over the years, the development of microwave metamaterial absorbers has turned towards compact, Lightweight, efficient designs that have multi-band and polarization insensitive features. Absorbers can now be adapted to a wide range of applications from telecommunication to sensing to stealth, through integration of metamaterials, novel materials and optimization techniques [36]. All these developments set the stage for new breakthroughs in electromagnetic interference mitigation, communication systems, and sensor technologies in the future [37-38].

In this presented work, an innovative triple-band polarization-insensitive microwave metamaterial absorber has been developed for electromagnetic interference (EMI) shielding and stealth applications targeting the S and C bands. This absorber, comprising a Flame Retardant 4 (FR-4) dielectric layer and a back-annealed copper layer, exhibits notable absorption peaks at 3.46, 4.98, and 7.26 GHz, achieving high absorption rates. It is unique in its structure because each resonator is designed with both open and closed loop structures. The combination offers excellent TE and TM absorption across a broad range of incident angles and polarization insensitivity. This absorber has a higher level of protection in the band [39] and offers significant protection of the RF signals, which is promising in terms of 5G networks and satellite communication.

2. ABSORBER UNIT CELL DESIGN

The proposed microwave metamaterial absorber consists of three layers: the ground layer, the substrate layer and the design layer. The ground layer is coated with a material that is an annealed copper, giving improved conductivity. The two metallic layers are separated by a lossy dielectric layer which is formed with FR-4, a standard substrate material, which is strong and has a low cost. The relative permittivity of the dielectric is 4.4 and its loss tangent is 0.02 and is 1.6mm thick. The uppermost section of the designed unit cells is a complex pattern of multiple rectangular sections, with several lines and gaps connecting the sections. It is very structured, almost like a maze, and the rectangles are nested to create a complex symmetrical structure. The absorber is probably designed to resonate with the electromagnetic waves, and the lengths of the paths (a1, a2, b1, b2, b3, etc.) and gaps (g1, g2) are adjusted to create the desired absorption characteristics. This configuration enables the effective absorption of electromagnetic waves in desired frequency bands. The absorber unit cell layout is a complex geometry as shown in Fig. 1(a). The top view of the developed triple-band microwave metamaterial absorber is presented in Fig.1(b) and the perspective view of the proposed structure in Fig. 1(c). A careful selection of materials and layering techniques provides the designed absorber with optimal performance for a number of applications where electromagnetic interference is to be mitigated. Table 1 provides an outline of the key dimensions of the unit cell design.

TABLE 1. Proposed Microwave Metamaterial Absorber Design Dimensions

Parameter	Value (mm)	Parameter	Value (mm)
p	11.7	b_1	4.9
a_1	11.6	b_2	5.4
a_2	10.9	b_3	4.2
a_3	10.5	b_4	1.1
a_4	9.8	b_5	2.2
a_5	9.1	g_1	2.5
a_6	8.6	g_2	0.2
a_7	2.2	h	0.2
t_c	0.035	t_{sub}	1.6

The absorption ability of the microwave absorber is determined by [34],

$$A(\omega) = 1 - |S_{11}|^2 - |S_{21}|^2 \quad (1)$$

Thus, reducing the reflectivity and transmissivity is essential to achieve almost unity absorption. It has solved the transmission problem by providing the absorber with a copper material which eliminates all transmission. Hence the backside of the substrate in the unit cell is covered with copper to block any electromagnetic power transfer and hence the transmission becomes negligible. So Eq. (1) becomes,

$$A(\omega) = 1 - |S_{11}|^2 \quad (2)$$

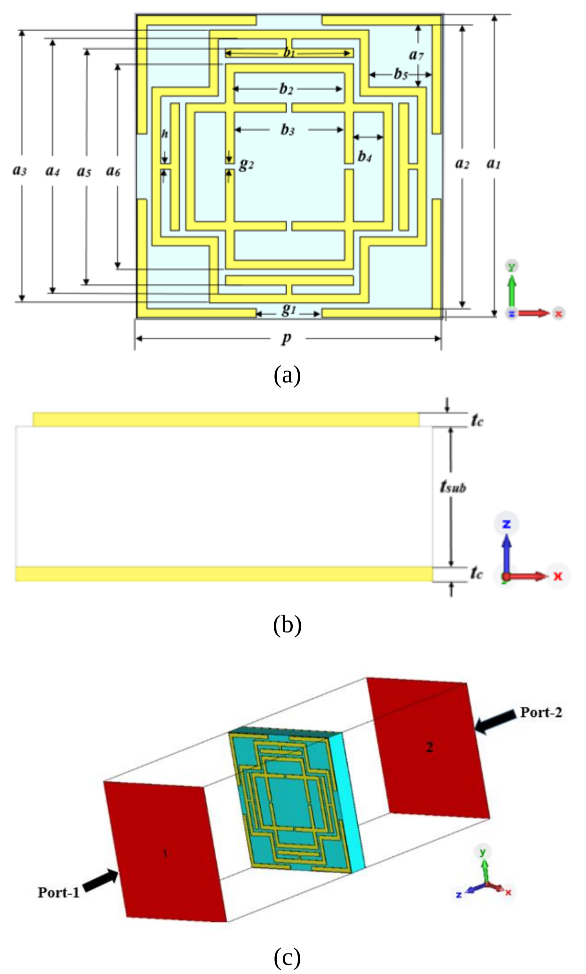

FIGURE 1. (a) Top, (b) Side, and (c) Perspective views of the proposed microwave metamaterial absorber.

It can be seen from Eq. (2) that the absorption approaches to near unity with decreasing reflection coefficients. The design of the structure is refined to allow the effect of the signal to absorb without reflection. This way, the signals are more effectively picked up and used, improving the overall efficiency of the absorber design. Furthermore, better performance is achieved by removing reflections, which also reduces unwanted interference and signal degradation [18].

$$Z(\omega) = \sqrt{\frac{(1+S_{11})^2 - S_{21}^2}{(1-S_{11})^2 - S_{21}^2}} \quad (3)$$

where,
Z(ω) is the impedance transformation
S_{11} represents the reflection coefficient value at port 1
S_{21} denotes the transmission coefficient via port 1 to port 2

Since the back of the absorber is coated with copper material there will not be any transmission of the signal ensuring transmission to be zero. The result Z(ω) demonstrates the structure's impedance characteristics at the selected frequency. Use this knowledge to investigate or design impedance matching networks to achieve optimal absorption results. Therefore, the Eq. (3) can be written as,

$$Z(\omega) = \frac{1+S_{11}}{1-S_{11}} \quad (4)$$

Shielding effectiveness (SE) is an important factor that determines how well a metamaterial unit cell absorbs electromagnetic radiation at a specific frequency. The effectiveness of an EMI shielding system determines its performance. Maxwell's equation contributes to the understanding of EMI shielding [44]. The total SE was determined using a logarithmic scale and the following equation [39]:

$$SE(dB) = SE_R + SE_A + SE_{MIR} \quad (5)$$

Because of the high frequency range (over 1 GHz), MIR loss is often avoided. Therefore, the Eq. (5) can be written as,

$$SE(dB) = SE_R + SE_A \quad (6)$$

Using the scattering parameters in the next formulas to compute reflection and absorption loss.

$$SE_R = 10\log\left(\frac{1}{1-S_{11}^2}\right) = 10\log\left(\frac{1}{1-R}\right) \quad (7)$$

$$SE_A = 10\log\left(\frac{1-S_{11}^2}{S_{21}^2}\right) = 10\log\left(\frac{1-R}{T}\right) \quad (8)$$

Adding Equations (7) and (8) to Equation (6) yields the overall EMI shielding effectiveness:

$$SE(dB) = 10\log\left(\frac{1}{1-R}\right) + 10\log\left(\frac{1-R}{T}\right) \quad (9)$$

SE(dB) offers insight into power transmission through the EMI shield. Higher SE values indicate more effective shielding.

3. RESULTS AND DISCUSSION

3.1 EVOLUTION OF DESIGN CONCEPT

As seen in Figure 2, the triple-band absorber design method comprises five stages. Stage I served as the original inspiration for the proposed unit cell. When it comes to geometric or design concepts, starting with a basic foundational step makes it easier to understand how intricate patterns or structures are put together. It also acts as a point of reference for comparing modifications and comprehending the fundamental symmetry or recurrence in the design procedure [40-41].

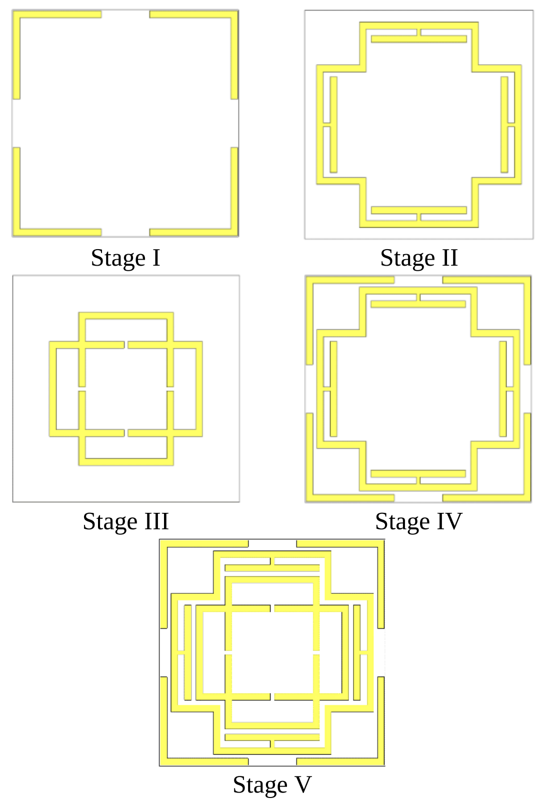

FIGURE 2. Multiple phases of the suggested triple-band absorber unit cell structure.

The dielectric substrate FR-4 of stage I to stage V (Proposed) has maintained a thickness of 1.6 mm, and its top layer's resonant pattern is drafted with a fractal geometry in an effort to make the proposed absorber unaffected to the polarization angle of EM waves. Figure 3 displays the absorptivity curve for the proposed unit cell design at various stages when both polarization and oblique angle of incidences are fixed at 0^{o}. At stage I, the unit cell achieves only one band, which appears at 8.54 GHz, and the absorptivity at this stage is only 73%. The degradation of an incoming EM wave mainly happens due to dielectric loss in the material itself.

Stage II of the unit cell also failed to achieve a triple band, providing only a single band with 93% absorptivity at 3.84 GHz. To increase the number of bands of the proposed absorber structure, interlocking squares are added to the structure on the inner side of the structure as stage III achieves more than 97% absorption at 5.24 GHz. However, the absorption in the desired range remains restricted to a single band only. To, even more, increase the number of bands, stage I and stage II are combined to get stage IV, which achieves two bands at 3.54 and 7.23 GHz with 90% and 97% absorption. But it has yet to achieve the design idea of covering the S and C bands. Finally, by combining stages III and IV, the unit cell's final structure achieves 97% absorption at 3.46 GHz, nearly unity absorption response at 4.98 GHz, and 96% at 7.26 GHz. The proposed microwave metamaterial absorber exhibits bandwidths of approximately 90, 120 and 150 MHz indicative at 3.46, 4.98 and 7.26 GHz, respectively. Figure 4 shows the simulated shielding effectiveness response of the developed triple-band absorber unit cell. It has shielding effectiveness values of 36 dB, 104 dB, and 35 dB for the three absorption frequencies: 3.46 GHz, 4.98 GHz, and 7.26 GHz, respectively.

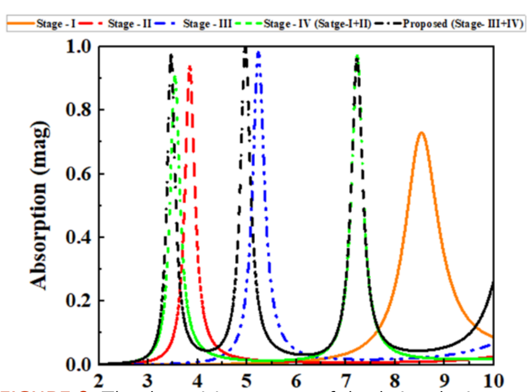

FIGURE 3. The absorptivity response of the designed microwave metamaterial absorber structure at various stages.

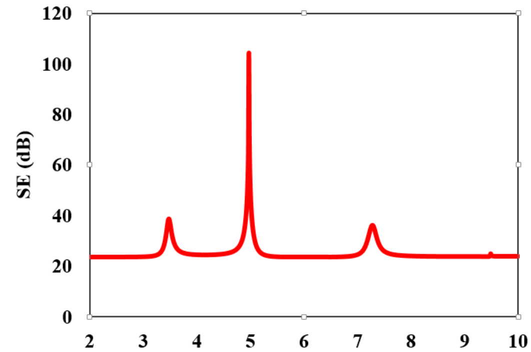

FIGURE 4. Shielding effectiveness results of the proposed triple-band absorber structure.

3.2 EFFECT OF GAPS g1 AND g2 ON THE ABSORPTIVITY

The proposed microwave metamaterial absorber structure is examined for modifications to the unit cell design parameters so as to better explore the absorption response. This section demonstrates the numerical results obtained for various physical dimensions of the proposed absorber design. Parametric evaluations were conducted on essential parameters to arrive at the proposed design. The impact of the gap *g1* between the adjacent segments of the outer square structure and gap *g2* between the two consecutive parts of the inner square of the unit cell on the absorption is illustrated in Figure 5. The gaps *g1* and *g2* affect the capacitance between the outer and inner square's consecutive parts. A smaller *g1* and *g2* increase capacitance due to stronger electric field coupling between segments. Additionally, the electromagnetic interaction between various structural components is influenced by the gaps *g1* and *g2*.

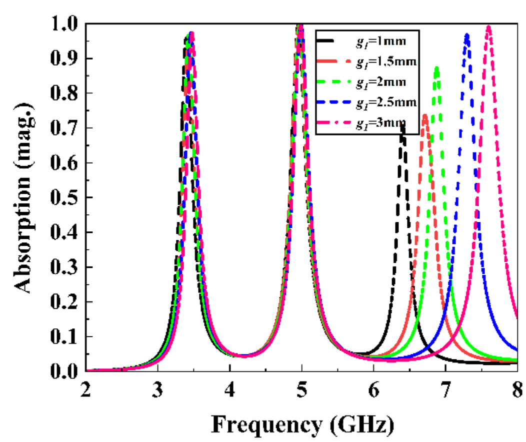

(a)

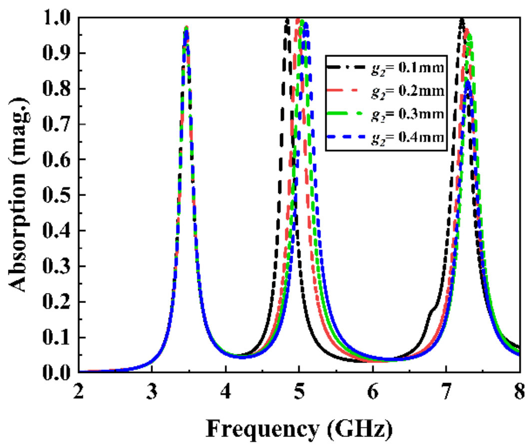

(b)

FIGURE 5. Unit cell absorption characteristics were developed to address variation in the gaps (a) Gap g_1 (b) Gap g_2.

The distribution and absorption of energy across the structure are impacted by variations in coupling, which modifies the resonant frequencies. The arrangement and spacing of the conducting elements impact the structure's inductance. Changing *g1* can marginally affect current pathways and magnetic coupling. As *g1* reduces, capacitance rises, leading to a decrease in the central resonant frequency. In contrast, increased *g1* reduces capacitance and increases the central resonant frequency. Keeping all other parameters constant, the absorbance peaks shift toward higher frequencies when *g1* increases from 1 to 3 mm in 0.5 mm increments. This is in line with capacitance decreasing as the gap expands. The increase in g1 value also leads to increases in the absorption magnitude. Figure 5(a) illustrates the absorption characteristics to address variation in the gap *g1* of the structure. Similar to *g1*, modifications to *g2* would cause the resonant peaks to shift. The *g1* rises from 0.1 to 0.4 mm in 0.1 mm increments while maintaining all other parameters constant, as shown in Table 1. The absorption peaks would move rightward to greater frequencies with a larger *g2* and towards lower frequencies with a smaller *g2*. Figure 5(b) illustrates the absorption characteristics to address variation in the gap *g2* of the structure.

3.3 THE IMPACT OF POLARIZATION ANGLE VARIATIONS

The simulations utilized the frequency domain solver of the commercial software CST [45] to continuously improve the absorber's geometric parameters, adopting unit cell boundaries. The unit cell boundaries were used in the x-and y-axes, with an open boundary along the z-axis. The incoming EM wave was polarized in the z-axis. The Floquet port was used to excite the unit cell and the scattering parameters were obtained from the two lowest Floquet modes (TE and TM). The convergence was controlled through the criterion $\Delta S \leq 0.01$ in two consecutive passes and a local refinement around the narrow coupling gaps g1 and g2 and around the metallic edges, using a tetrahedral adaptive mesh with the highest frequency of about 15 mesh cells per wavelength. The copper layers were modelled with conductivity $\sigma = 5.8 \times 10^7$ S/m and the structure was solved over 2 – 10 GHz with adaptive frequency sampling to solve the three resonances. When developing a microwave metamaterial absorber, it is crucial to maintain a wide oblique incidence angle and wide polarization angle absorption characteristics. In the TE mode, the wave component moves along the z-axis, while the electric field vector moves along the x-axis and the magnetic field vector moves along the y-axis. In contrast, the z-axis of the electromagnetic field vector contains a component of the magnetic field (H-field), denoted as Hz. In the TM mode, the electric field vector (Ez) has components along the z-axis, whereas the magnetic field vector (Hx) and electric field vector (Ey) are aligned with the x- and y-axes, respectively.

Figure 6 illustrates the identical absorption response of the normal incidence of EM wave for variation in polarization angles for the TE mode. The suggested absorber structure has strong axial symmetry, resulting in a stable absorption slope that is unaffected by the polarization incidence variations. The proposed microwave metamaterial absorber structure's polarization-independent behaviour can be theoretically explained through its four-fold structural symmetry. In this analysis, the wave propagation direction remains fixed, while the electric (E) and magnetic (H) fields rotate with an angle φ. The study adjusts the polarization angle φ, which ranges from 0 to 90 degrees in 30-degree steps.

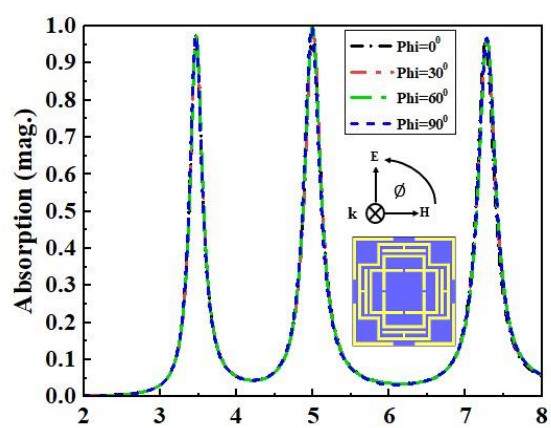

FIGURE 6. Absorption characteristics of the developed unit cell in the TE mode over multiple polarization (ϕ) angles.

The developed unit cell attains the three absorption bands with center frequencies of 3.46, 4.98 and 7.26 GHz with absorption efficiency of 97%, near unity absorption (99.8%), and 96%, respectively. The developed microwave metamaterial absorber structure exhibits a nearly identical response for all three central absorption frequencies. This uniform absorption performance showcases the durability and effectiveness of the developed unit cell structure, suggesting its potential applications across various fields where efficient electromagnetic absorption is desired. Figure 6 also demonstrates complete polarization insensitivity, as the absorption responses remain consistent despite variations in polarization angles.

3.4 THE IMPACT OF OBLIQUE ANGLE VARIATIONS

In real-world applications, electromagnetic (EM) waves encounter oblique angles when interacting with the surface of microwave metamaterial absorbers. In order to delve deeper into the absorption characteristics of the suggested microwave metamaterial absorber, we extend our analysis to explore how absorption properties vary with the angle of incidence, denoted as θ, which represents the angle among the propagation vector and the z-axis. The current goal is to adjust the axis of rotation to a range that covers the S- band and C-band for all incident angle ranges. Figure 7(a) and 7(b) show the absorption characteristics for the TE and TM modes at distinct angles of oblique incidence. The implemented unit cell provides a very good absorption performance for orientations up to 60^o. In the Transverse Electric mode, when the oblique angle rises, the initial and middle absorption nulls slightly shift to high-frequency values, and the last absorption null moves to a lower frequency range, i.e., shifting leftwards. This is since the wave's effective travel length through the material or structure increases. This indicates that the wave goes longer into the material, altering the phase and causing the resonance frequency to affect. The absorption rates for the first and second frequency peaks attains more than 90% even when the angle changes, but the absorption rate is reduced to 80% for the third absorption peak. In Transverse magnetic mode, the absorption characteristics change when the incident angle changes obliquely to15^o. As the oblique angle rises to 60^o, the first and second absorption nulls show very little shift in their frequency range, but the third absorption null, i.e., 7.26 GHz, shifts to the higher frequency range. All of the absorption nulls of the implemented unit cell achieve an absorption rate of more than 95% at an oblique angle of 60^o. These obtained results confirm that the proposed unit cell exhibits a wide angular performance for oblique incidence waves.

The absorption response observed in Figure.7 can be further clarified by the angle dependence of wave impedance observed with TE and TM polarizations. Under normal incidence both the polarizations behave similarly. At an oblique angle of incidence, the free space impedance becomes $Z_o/_{cos\theta}$ for TE polarized wave and becomes $Z_o cos\theta$ for TM polarized wave. The Z_0 value is approximately 377Ω. When the θ increases, impedance of TE wave increases and TM wave decreases. As a result the impedance matching condition of the absorber for TE and TM modes varies slightly as the incidence angle increases.

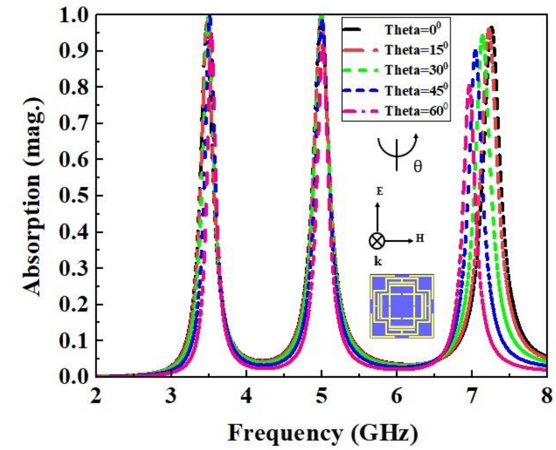

(a)

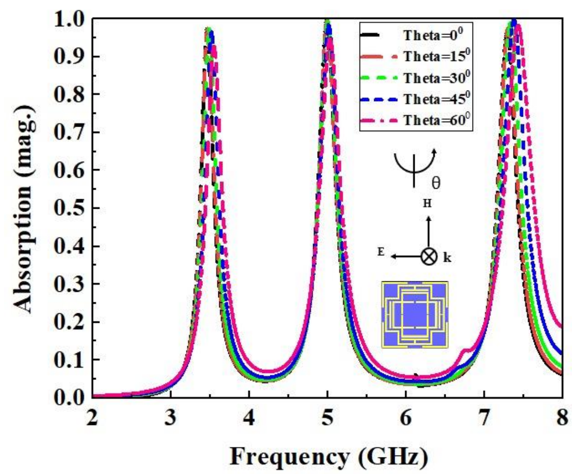

(b)

FIGURE 7. Absorption characteristics of the developed unit cell simulated over multiple oblique angles in the (a) TE mode and (b) TM mode.

In this study of microwave metamaterial absorbers, we have observed significant absorption performance characterized by theta values of up to 60^o across frequencies of 3.46, 4.98 and 7.26 GHz. The strong absorptivity across different theta angles indicates the broad applicability of the absorber in practical scenarios where different types of electromagnetic radiation are encountered. The results presented here indicate potential for this absorber in practical applications that require efficient absorption over a range of frequencies and incident angles, leading to better performance and reliability in the corresponding systems and technologies.

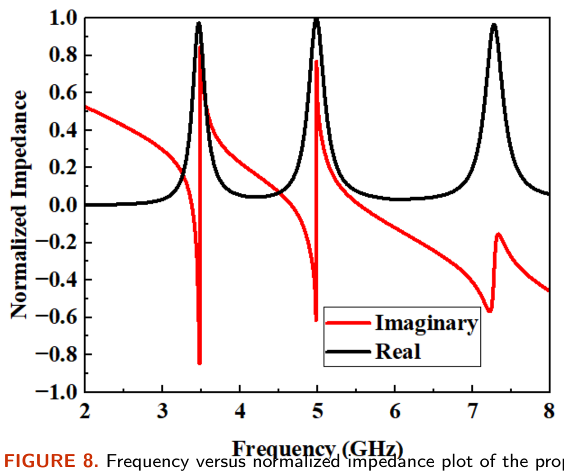

FIGURE 8. Frequency versus normalized impedance plot of the proposed microwave metamaterial absorber.

The normalized impedance in the proposed three band microwave metamaterial absorber is shown in Figure 8. As seen in the Figure 8, the real part of the impedance curve is close to unity at three frequencies: 3.46 GHz, 4.98 GHz and 7.26 GHz. When the impedance of the absorber is matched to that of free space, there is minimal reflection and more energy absorbed at the boundary between absorber and free space. In addition, at these frequencies, the imaginary part of the impedance curve quickly approaches zero, which indicates that the impedance of the load is very close to that of the transmission line and of the free space. The non-zero imaginary part shown in Figure 8 is due to the capacitive reactance of the resonator elements. The gap capacitances (g1 and g2) created by the resonators cause the negative values in Figure 8. At each resonance the reactance of the structure alternates between being inductive and being capacitive, and at the matched frequency, the reactance is zero. From the shape of the impedance curve, it is evident that the proposed absorber is carefully engineered to enable significant absorption effects over a range of frequencies by carefully controlling the dimensions of the structure.

3.5 EQUIVALENT CIRCUIT MODEL

The triple-band microwave metamaterial absorber can be represented by its transmission line model as shown in the Figure 9(a), corresponding equivalent circuit design, to evaluate the electromagnetic properties of the absorber. The patches inside the metamaterial resonators are represented by resonant branches (R-L-C), which enable the generation of different resonant frequencies in the unit cell structure [43]. The suggested unit cell configuration is a set of three parallel RLC branches, each of them tuned to a different resonant frequency that helps to absorb the frequencies at a certain frequency band. The parallel capacitors (*C4, C5, and C6*) are in the circuit to help couple the capacitance between the resonators of the unit cell. These capacitors are important to ensure that the free space impedance equals the input impedance of the unit cell at its resonant frequencies. The terminals inductor L4 is similar to a metallic ground plane as it has a metal back substrate like a short circuit transmission line. The software Advanced Design System (ADS) optimizes the suggested lumped circuit model and the values of the components are given in [42] and are shown in Table 2. The comparison of the simulated value of $|S_{11}|$ for the proposed microwave metamaterial absorber is displayed in Figure 9(b) using ADS (black curve) and CST (red curve).

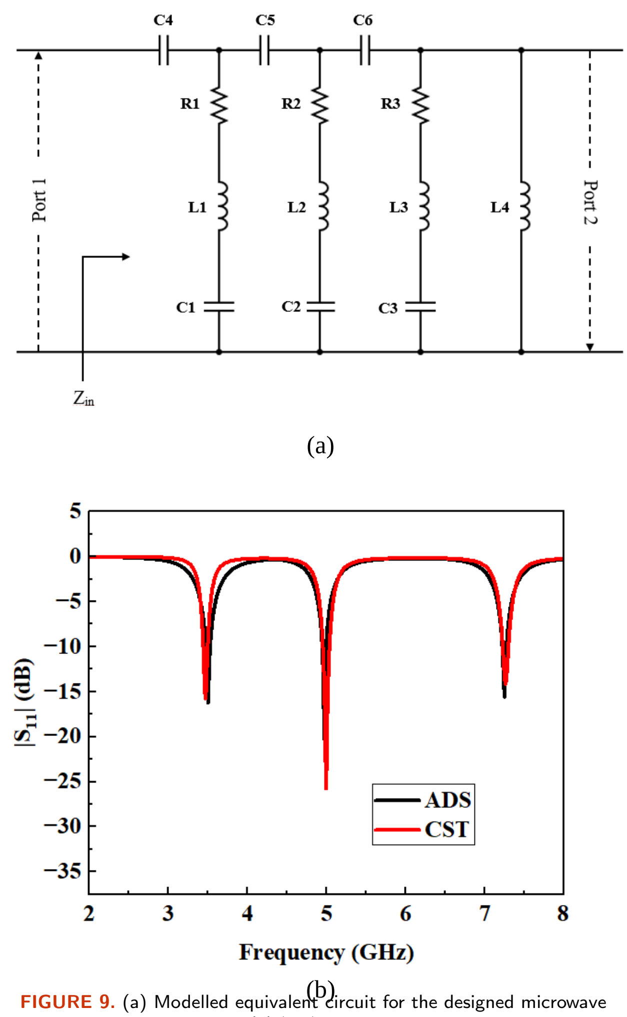

FIGURE 9. (a) Modelled equivalent circuit for the designed microwave metamaterial absorber, and (b) $|S_{11}|$ comparison between the equivalent circuit (ECM) results and the simulation results.

TABLE 2. Component values of the proposed microwave metamaterial absorber

Component	Value	Component	Value
R_1 (Ω)	69.97	C_1 (pF)	0.016
R_2 (Ω)	36.61	C_2 (pF)	0.077
R_3 (Ω)	40.05	C_3 (pF)	0.058
L_1 (nH)	30.097	C_4 (pF)	2.018
L_2 (nH)	27.2068	C_5 (pF)	0.1
L_3 (nH)	26.801	C_6 (pF)	0.01
L_4 (nH)	100	–	–

3.6 INVESTIGATION OF THE ABSORPTION MECHANISM

The proposed mechanism for absorption in the triple-band microwave metamaterial absorber is analyzed under TE wave excitation. This is accomplished by analyzing the E- and H-field distributions along with surface currents. Figures 10(a) to 10(c) illustrate the distributions of the relative H-field, E-field, and surface current at a frequency of 3.46 GHz. The distribution of the electric field is predominantly localized on the vertical segments of the central interlocked structure. Conversely, at the same frequency, the distribution of the magnetic field (H-field) is primarily found on the horizontal segments of the central structure. Notably, the surface current flows in a direction that is precisely opposite to that of the electric field generated by the incident TE wave, suggesting that electrical resonance plays a significant role in the absorption mechanism.

At 4.98 GHz, all the fields are concentrated on the innermost interlocked square structure. For E-field distributions, the signal mainly resides in the vertical segments. The signal focused on the horizontal segments of the innermost interlocked square structure for the H-field along with surface current. Figures 10(d) through 10(f) show the field distributions at 7.26 GHz. For 7.26 GHz, the signal was primarily based on the outermost square structure. The E-field distributions are focused on the vertical segments. The signal predominantly focused on the horizontal segments of the outermost square configuration concerning the distributions of the H-field and surface currents.

Figures 10(g) to 10(i) present the distributions at a frequency of 7.26 GHz. Additionally, the physical behavior of the proposed triple-band absorber unit cell is examined under Transverse Magnetic (TM) wave excitation. Figures 11(a) to 11(i) illustrate the distributions of the relative electric field (E-field), magnetic field (H-field), and surface current at frequencies of 3.46, 4.98, and 7.26 GHz, respectively. The E-field distributions are predominantly localized on the horizontal segments of the structure, while the H-field and surface current distributions are primarily located on the vertical segments. The above field analysis was performed on the unit cell with periodic boundary conditions, which will automatically model the mutual coupling that will occur between every cell in an infinite periodic array. The inner cells of this electrically large fabricated 26 × 26 array are well approximated by this periodic environment and the coupling effects are primarily the outermost edge cells. The field distributions in the unit cells are, therefore, characteristic of the behavior of the fabricated array.

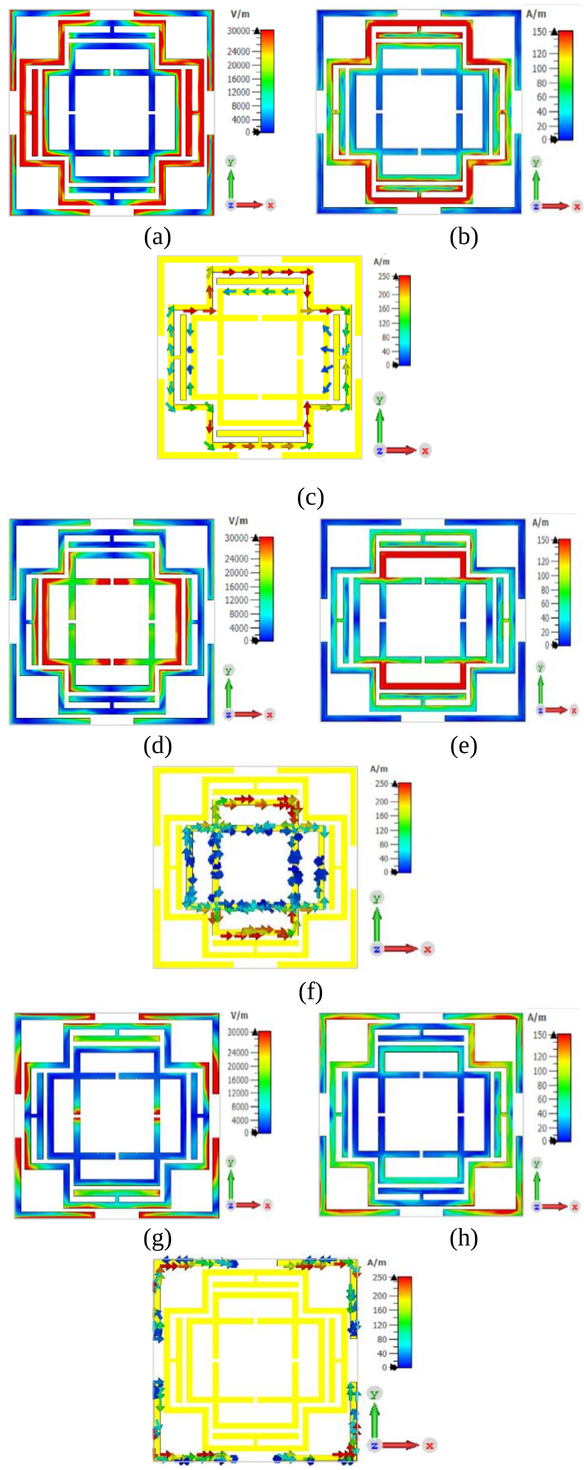

FIGURE 10. E-field, H-field and surface current distributions on the top layer of the structure at 3.46 GHz (a)–(c), 4.98 GHz (d)–(f) and 7.26 GHz (g)–(i) under TE wave excitation.

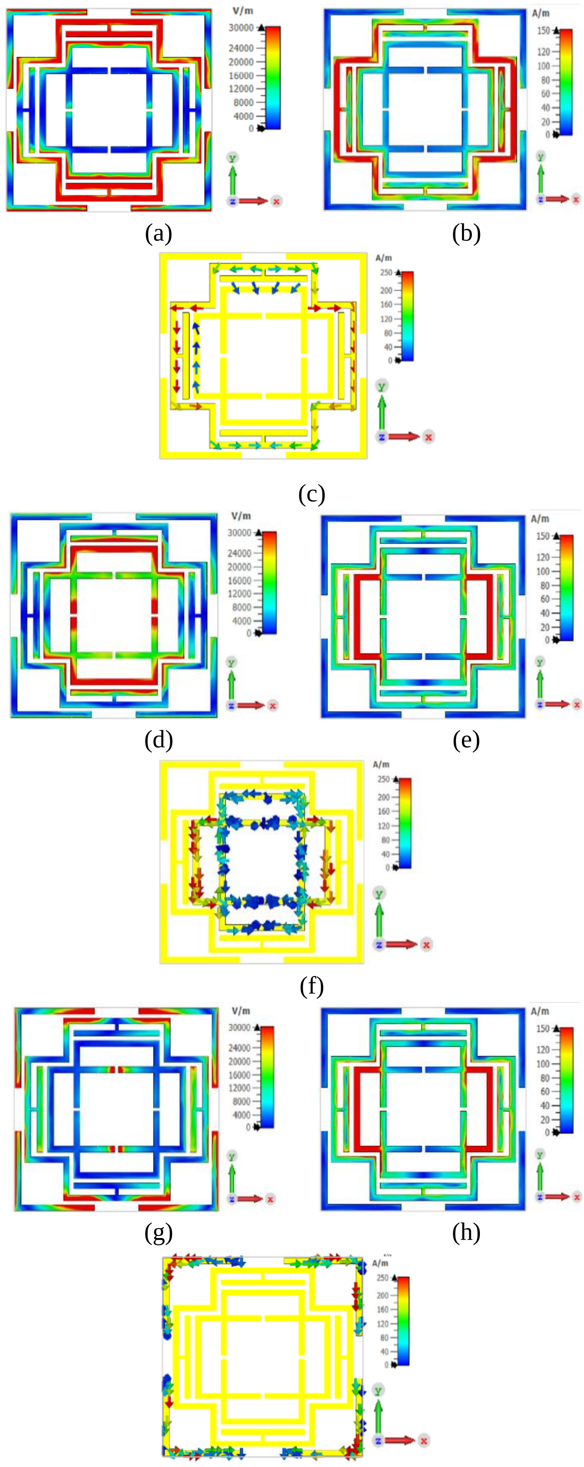

FIGURE 11. E-field, H-field and surface current distributions on the top layer of the structure at 3.46 GHz (a)–(c), 4.98 GHz (d)–(f) and 7.26 GHz (g)–(i) under TM wave excitation.

4. MEASUREMENT RESULTS

The proposed unit cell was printed as a 26 × 26 array (304.2 mm × 304.2 mm) on the top copper layer. The 26 x 26 size was chosen as a balance between electrical size and measuring feasibility. The array size of 304.2 mm × 304.2 mm exceeds $3.5\lambda_0$ at the lowest resonance frequency (3.46 GHz), allowing for infinite-array behavior. At a measurement distance of 1.18 m, the plane wave propagation area of the horn antenna is small, further reducing edge diffraction. A larger array would add more expense in fabrication and handling of the substrates without any significant improvement in the measured absorptivity. This approach uses FR-4 epoxy substrates that are 1.6 mm thick. A 35 µm thin copper layer is deposited on each side of the substrate material. The experiment was done with two VERDANT JR 12 type horn antennas. The primary horn-type antenna was linked to port-1 of a Keysight Microwave analyzer N9951A via a low-loss coaxial cable, while the additional horn-type antenna was attached to port-2 to capture the reflected wave. The device was positioned 1.5 meters high from the ground and the prototype sample was placed 1.18 meters away from the antennas to prevent near-field impacts. These distances were chosen to keep the absorber in the far-field of the horn antenna. The brightness of the sample at a distance of 1.18 m resembles a plane wave, as assumed in the unit-cell simulation. The closer the sample is put, the worse the correlation between experiments and modelling because the wavefront is bent and the light throughout the array varies. Because of the finite distance and angle of 50° between the transmitting antenna and receiving antenna, a little discrepancy in peak absorptivity is detected between the simulated and measured results, as shown in Figs. 13-14. The entire measurement process tool place within an anechoic chamber. First, the copper plate's reflection is measured and then the fabricated absorber is subsequently set in the correct location and tested again.

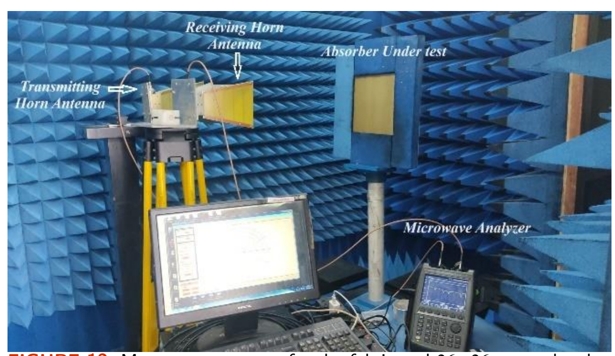

FIGURE 12. Measurement setup for the fabricated 26×26 array absorber in reflectance mode at a separation angle of 50°.

TABLE 3. Observed Absorptivity of the Fabricated Triple-band Absorber null frequencies at Polarization and Oblique angle of Incidence for TE mode and TM mode.

Polarization angle at 0°				Oblique angle at 0°			
TE		TM		TE		TM	
f (GHz)	Abs. (%)	f (GHz)	Abs. (%)	f (GHz)	Abs. (%)	f (GHz)	Abs. (%)
3.44	91.8	3.50	88.2	3.46	88.1	3.47	88.7
5.00	96.7	5.05	96.4	5.04	93.0	5.03	95.5
7.26	90.4	7.39	90.6	7.34	94.4	7.27	91.4

Table 3 presents the absorptivity values for the measured null frequencies of the triple band absorber, assessed under normal polarization along with the oblique angles of incidence for both TE and TM polarized waves.

The actual reflection was computed by subtracting the power reflected from both the test apparatus and the copper plate. Subsequently, the absorptivity was ascertained utilizing the reflection coefficient. A good degree of consistency between the simulations and the experimental results is observed during comparison. The measurement result indicates a triple-band response at 3.44, 5, and 7.26 GHz, respectively, with a maximum absorption rate of 91.8%, 96.7%, and 90.4%.
The absorption spectrum data for TE and TM modes under polarization angles are compared between simulated and observed in Figure 13, revealing nearly identical results with only a small shift in frequency null. Frequency shifts are caused by resistance tolerance, sample fabrication tolerance, measurement setup, and substrate dielectric dispersion. The most tolerance-sensitive gaps are g1 (2.5mm) and g2 (0.2mm). This is because the resonant frequencies are dependent upon the gap capacitance. When the etching tolerances are larger, the resonances will shift. This is in line with the small offsets observed in Figs. 13–14. Four-fold symmetry makes the design robust to over- or under-etching. With all four arms moving together, the polarization-insensitive response remains unaffected. The choice of FR-4 was made due to its abundance and low cost. The relative permittivity of FR-4 slightly varies from sheet to sheet, and its loss tangent increases with frequency. These variations can cause the resonant frequencies to shift and alter the absorption levels, especially at the highest resonant band. Here, the absorption is determined by the dielectric loss. As a result, the higher value of loss tangent at the highest resonant frequency leads to a wider and partially reduce the resonance. Rogers, a low-loss material, would be more consistent at high frequencies, but it is more expensive. Figure 14, illustrates the simulated and experimental absorption characteristics of the oblique angle of incidence varies from 0° - 60° by keeping the polarization angle of 0° under TE mode and TM mode. To measure the transmission coefficient, the transmitting horn antenna and metasurface absorber were kept at a distance of about 1.18 meters, and the absorber and receiving antenna were kept at a distance of 0.58 meters.

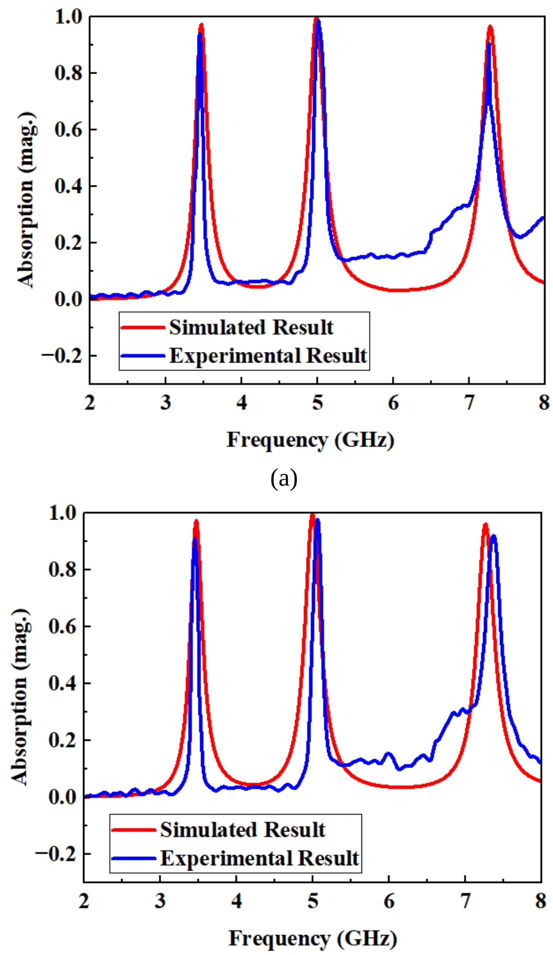

(b)

FIGURE 13. Validation of absorption experimental outcomes with the simulated results at $\theta = \phi = 0^\circ$ polarization incident for (a) TE mode (b) TM mode.

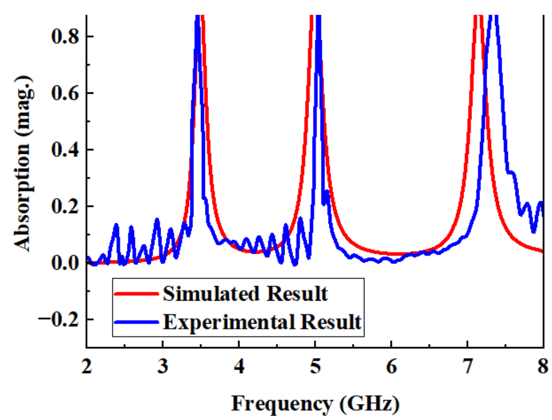

(a)

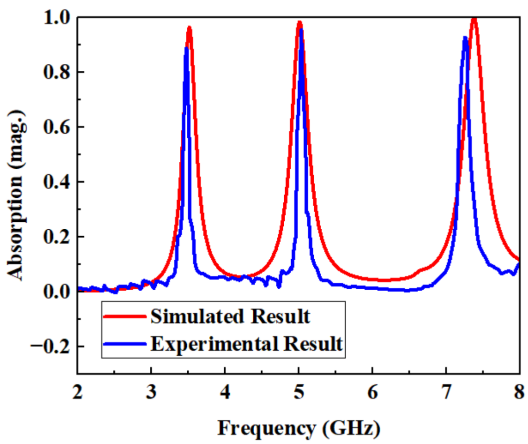

(b)

FIGURE 14. Validation of Absorption experimental outcomes with the simulated results at $\phi = 0°$, $\theta = 45°$ oblique incident for (a) TE mode (b) TM mode.

Table 4 compares the proposed work with the existing microwave metamaterial absorbers. The proposed structure has a nested geometry with an amalgamation of open and closed loop resonators. This structural novelty has brought in three significant performance developments of the proposed absorber as evident from the comparison table (Table 4) given in the manuscript: (i) the unit cell has the most compact size; (ii) best performance under oblique incidence inspite of having triple absorption bands; (iii) completely polarization insensitive.

TABLE 4. The proposed work is compared with existing metamaterial (MM) absorbers

Ref.	Year	No. of bands	Resonating frequencies (GHz)	Absorption peaks (%)	Unit Cell Size (λ_o)	Dielectric thickness (mm)	Dielectric substrate	Oblique incident angle	Shielding Effectiveness (dB)	Polarization insensitivity	Application bands
[4]	2023	2	6.78 &13.92	91.73 & 99.97	$0.271\lambda_o^2$	1.52	FR-4	45°	-	Yes	C-band and Ku-band
[11]	2023	3	6.24, 10.60 & 18.62	97.8, 99.9 & 99.9	$0.166\lambda_o^2$	0.58	Rogers RO4003C	-	-	No	C band, X band and K band
[13]	2022	3	2.4, 5.2 & 5.8	99, 98 & 98	$2.669\lambda_o^2$	3.07	FAB*	-	-	No	Wi-Fi bands
[18]	2022	3	5, 6.88 & 8.249	-	$0.166\lambda_o^2$	1.6	FR-4	-	-	No	C- band and X-band
[23]	2024	2	2.38 & 5.81	99 & 90	$0.79\lambda_o\times 0.63\lambda_o$	0.7	FR-4	60°	-	Yes	ISM band
[33]	2022	2	4.10 & 4.96	99.99 & 99.57	$0.169\lambda_o^2$	1.6	FR-4	-	-	No	C-band
[34]	2023	3	5.86, 6.57 & 8.94	86.23, 92.92 & 82.07	$0.234\ \lambda_o^2$	0.8	FR-4	-	-	Yes	C- and X-band
[38]	2022	3	5.376,10.32 & 12.25	99.9, 99.9 & 99.7	$0.179\ \lambda_o^2$	1.6	FR-4	60°	**Yes (>40)**	Yes	C- band and X-band
[41]	2024	3	2.5, 5.2, 9.8, and 11.0	90, 91, 97 & 94	$0.18\ \lambda_o^2$	1.6	FR-4	60°	-	Yes	S, C, and X
[42]	2025	3	4.98,9.97,14.4	99.76,97.2,99.3	$0.15\ \lambda_o^2$	0.787	FR-4	60°	-	Yes	C- band, X-band and Ku-band
Proposed Work	**2025**	**3**	**3.46, 4.98 & 7.26**	**97, 99.8 & 96**	$\mathbf{0.134\ \lambda_o^2}$	**1.6**	**FR-4**	60°	**Yes (>35)**	**Yes**	**S-band and C-band**

FAB*-Floating Action Buttons, PET*-Polyethylene terephthalate, GML1000*- glycerol monolaurate 1000, λ_o is the wavelength corresponding to the lowest absorption frequency.

5. CONCLUSION

This paper presents a multiband polarization-insensitive microwave metamaterial absorber which performs effectively in EMI shielding and stealth applications specifically within the S and C frequency bands. Through meticulous design comprising an FR-4 dielectric layer and a back-annealed copper layer, the absorber achieves impressive absorption peaks at 3.46, 4.98, and 7.26 GHz, with absorption levels exceeding 96% across all bands under normal incidence. The absorber maintains an absorption efficiency of over 80% even when the incident angle is up to 60% for TE mode and TM mode, which demonstrates its excellent performance in practical applications. This absorber is effective at reducing the impact of RF signals on sensitive devices that are vulnerable to electromagnetic impact over the band, confirming its shielding performance. Besides simulation, an equivalent circuit of parallel RLC resonators was designed to analyze the frequency response of the absorber. The physical behaviour of the absorber is clearly understood in this circuit and it is very similar to the simulation results. Analysis of the E-field, H-field and surface current indicates that the absorption mechanism is due to the strong electric and magnetic resonances that occur in specific resonator regions at each peak. In addition, the absorber comprising 26 × 26 unit cells was fabricated, and the reflection coefficient |S11| was measured and compared with the simulation results, demonstrating agreement between the two. Possible future modifications include tunable absorbers by using varactor or PIN diodes, active FSS designs for wider bands using lumped resistive loadings and multilayer designs for additional bands or flexible substrates for conformal applications.

REFERENCES

[1] Z. EL-Wasif, T. Ismail, and O. Hamdy, "Design and optimization of highly sensitive multi-band terahertz metamaterial biosensor for coronaviruses detection," *Opt. Quantum Electron.*, vol. 55, no. 7, 2023, Art. no. 604, DOI: 10.1007/s11082-023-04906-6.

[2] Y. Kang, J. Wang, and H. Liu, "A dual-band polarization insensitive metamaterial absorber with a single square metallic patch for sensing application," *Plasmonics*, vol. 17, no. 2, pp. 449–456, 2022, DOI: 10.1007/s11468-021-01537-z.

[3] K. S. L. Al-Badri, A. S. Younes, and K. F. Mamoon, "Ultra-thin dual-band perfect metamaterials absorber for microwave applications," *Mater. Today Proc.*, vol. 42, pp. 2164–2168, 2021, DOI: 10.1016/j.matpr.2020.12.300.

[4] M. Berka, U. Özkaya, T. Islam, M. El Ghzaoui, S. Varakumari, S. Das, and Z. Mahdjoub, "A miniaturized folded square split ring resonator cell based dual band polarization insensitive metamaterial absorber for C- and Ku-band applications," *Opt. Quantum Electron.*, vol. 55, no. 8, 2023, Art. no. 699, DOI: 10.1007/s11082-023-04954-y.

[5] X. Huang, H. Yang, S. Yu, J. Wang, M. Li, and Q. Ye, "Triple-band polarization-insensitive wide-angle ultra-thin planar spiral metamaterial absorber," *J. Appl. Phys.*, vol. 113, no. 21, 2013, Art. no. 213516, DOI: 10.1063/1.4809655.

[6] M. Bennaoum, M. Berka, A. Bendaoudi, A. Y. Rouabhi, and Z. Mahdjoub, "Investigation of a near-perfect quad-band polarization-insensitive metamaterial absorber based on dual-T circular shaped resonator array designed on a silicon substrate for C-, X- and Ku-bands applications," *Silicon*, vol. 15, no. 2, pp. 699–712, 2023, DOI: 10.1007/s12633-022-02038-2.

[7] S. Sakib, A. Hoque, S. K. B. A. Rahim, M. Singh, N. M. Sahar, M. S. Islam, M. S. Soliman, and M. T. Islam, "A central spiral split rectangular-shaped metamaterial absorber surrounded by polarization-insensitive ring resonator for S-band applications," *Materials*, vol. 16, no. 3, 2023, Art. no. 1172, DOI: 10.3390/ma16031172.

[8] M. S. U. Afsar, M. R. I. Faruque, M. B. Hossain, and M. T. Islam, "SRR inspired modified psi shaped perfect metamaterial absorber for C-band application," *J. Magn. Magn. Mater.*, vol. 582, 2023, Art. no. 171010, DOI: 10.1016/j.jmmm.2023.171010.

[9] G. Sen, A. Ghosh, M. Kumar, S. N. Islam, and S. Das, "A co-polarized microwave absorber with dual mode resonance based on dual split ring geometry for Wi-MAX and WLAN applications," *Prog. Electromagn. Res. M*, vol. 86, pp. 145–152, 2019, DOI: 10.2528/PIERM19080804.

[10] M. M. Hasan, M. R. I. Faruque, and M. T. Islam, "A tri-band microwave perfect metamaterial absorber," *Microw. Opt. Technol. Lett.*, vol. 59, no. 9, pp. 2302–2307, 2017, DOI: 10.1002/mop.30726.

[11] M. I. Jahan, M. R. I. Faruque, M. B. Hossain, and S. Abdullah, "An ultra-thin, triple-band, incident angle-insensitive perfect metamaterial absorber," *Materials*, vol. 16, no. 4, 2023, Art. no. 1623, DOI: 10.3390/ma16041623.

[12] M. S. U. Afsar, M. R. I. Faruque, S. Abdullah, and M. J. Hossain, "Rotational symmetric solar system shaped triple band perfect metamaterial absorber for S-, C-, and X-band application," *Sens. Actuators A Phys.*, vol. 365, 2024, Art. no. 114839, DOI: 10.1016/j.sna.2023.114839.

[13] Y. Wei, J. Duan, H. Jing, Z. Lyu, J. Hao, Z. Qu, J. Wang, and B. Zhang, "A multiband, polarization-controlled metasurface absorber for electromagnetic energy harvesting and wireless power transfer," *IEEE Trans. Microw. Theory Techn.*, vol. 70, no. 5, pp. 2861–2871, 2022, DOI: 10.1109/TMTT.2022.3155718.

[14] M. S. U. Afsar, M. R. I. Faruque, M. U. Khandaker, A. Alqahtani, and D. A. Bradley, "A new compact split ring resonator based double inverse epsilon shaped metamaterial for triple band satellite and radar communication," *Crystals*, vol. 12, no. 4, 2022, Art. no. 520, DOI: 10.3390/cryst12040520.

[15] M. Kaur and H. S. Singh, "Design and analysis of a compact ultrathin polarization- and incident angle-independent triple band metamaterial absorber," *Microw. Opt. Technol. Lett.*, vol. 62, no. 5, pp. 1920–1929, 2020, DOI: 10.1002/mop.32264.

[16] N. Mishra and R. K. Chaudhary, "Design and development of an ultrathin triple band microwave absorber using miniaturized metamaterial structure for near-unity absorption characteristics," *Prog. Electromagn. Res. C*, vol. 94, pp. 89–101, 2019, DOI: 10.2528/PIERC19043002.

[17] A. Elakkiya, S. Radha, B. S. Sreeja, and E. Manikandan, "An ultrathin microwave metamaterial absorber for C, X, and Ku band applications," *J. Electron. Mater.*, vol. 50, no. 12, pp. 7275–7282, 2021, DOI: 10.1007/s11664-021-09251-6.

[18] M. B. Hossain, M. R. I. Faruque, A. S. Ahmed, and M. T. Islam, "Wide bandwidth enriched symmetric hexagonal split ring resonator based triple band negative permittivity metamaterial for satellite and Wi-Fi applications," *Results Phys.*, vol. 37, 2022, Art. no. 105511, DOI: 10.1016/j.rinp.2022.105511.

[19] S. Genikala, A. Ghosh, and B. Roy, "Triple band single layer microwave absorber based on closed loop resonator structures with high stability under oblique incidence," *AEU Int. J. Electron. Commun.*, vol. 164, 2023, Art. no. 154629, DOI: 10.1016/j.aeue.2023.154629.

[20] M. A. Shukoor, V. Kumar, and S. Dey, "Compact polarisation insensitive wide angular stable triple band absorber for RF energy harvesting, RCS reduction, and sensor applications," *Int. J. RF Microw. Comput.-Aided Eng.*, vol. 31, no. 9, 2021, Art. no. e22763, DOI: 10.1002/mmce.22763.

[21] N. Kumar and B. K. Kuanr, "Single and double-layered tri-band microwave absorbing materials," *Ceram. Int.*, vol. 49, no. 20, pp. 32458–32469, 2023, DOI: 10.1016/j.ceramint.2023.07.204.

[22] O. F. Abdullah, O. A. Hussein, S. A. Shawkat, and K. S. L. Al-Badri, "Design double layers structure based dual band metamaterial absorbers for stealth applications," *J. Eng. Appl. Sci.*, vol. 14, no. 22, pp. 8315–8320, 2019, DOI: 10.3923/jeasci.2019.8315.8320.

[23] B. Tütüncü and Y. Altıntaş, "Dual-band polarization-insensitive high-efficiency metamaterial absorber for ISM-band biomedical applications," *J. Electron. Mater.*, vol. 53, no. 1, pp. 356–366, 2024, DOI: 10.1007/s11664-023-10776-1.

[24] A. S. Dhillon, D. Mittal, and R. Bargota, "Triple band ultrathin polarization insensitive metamaterial absorber for defense, explosive detection and airborne radar applications," *Microw. Opt. Technol. Lett.*, vol. 61, no. 1, pp. 89–95, 2018, DOI: 10.1002/mop.31547.

[25] P. Jain, A. K. Singh, J. K. Pandey, S. Bansal, N. Sardana, S. Kumar, N. Gupta, and A. K. Singh, "An ultrathin compact polarization-sensitive triple-band microwave metamaterial absorber," *J. Electron. Mater.*, vol. 50, no. 3, pp. 1506–1513, 2021, DOI: 10.1007/s11664-020-08680-z.

[26] S. A. Shawkat, K. S. L. Al-Badri, and I. Al-Barazanchi, "Three band absorber design and optimization by neural network algorithm," *J. Phys.: Conf. Ser.*, vol. 1530, no. 1, 2020, Art. no. 012129, DOI: 10.1088/1742-6596/1530/1/012129.

[27] M. A. Shukoor, S. Dey, and S. K. Koul, "A simple polarization-insensitive and wide angular stable circular ring based undeca-band absorber for EMI/EMC applications," *IEEE Trans. Electromagn. Compat.*, vol. 63, no. 4, pp. 1025–1034, 2021, DOI: 10.1109/TEMC.2021.3075730.

[28] P. Zuo, T. Li, M. Wang, H. Zheng, and E.-P. Li, "Miniaturized polarization insensitive metamaterial absorber applied on EMI suppression," *IEEE Access*, vol. 8, pp. 6583–6590, 2020, DOI: 10.1109/ACCESS.2019.2957308.

[29] R. Kubacki, W. Głuszewski, D. Laskowski, K. Rudyk, and M. Kuchta, "EMC microwave absorber for outdoor applications," *Int. J. Microw. Wireless Technol.*, vol. 10, no. 7, pp. 754–758, 2018, DOI: 10.1017/S1759078718000223.

[30] G. Deng, K. Lv, H. Sun, J. Yang, Z. Yin, Y. Li, B. Chi, and X. Li, "An ultrathin, triple-band metamaterial absorber with wide-incident-angle stability for conformal applications at X and Ku frequency band," *Nanoscale Res. Lett.*, vol. 15, no. 1, 2020, Art. no. 217, DOI: 10.1186/s11671-020-03448-0.

[31] S. Kalraiya, R. K. Chaudhary, and R. K. Gangwar, "Polarization independent triple band ultrathin conformal metamaterial absorber for C- and X-frequency bands," *AEU Int. J. Electron. Commun.*, vol. 135, 2021, Art. no. 153752, DOI: 10.1016/j.aeue.2021.153752.

[32] A. K. Singh, M. P. Abegaonkar, and S. K. Koul, "Dual- and triple-band polarization insensitive ultrathin conformal metamaterial absorbers with wide angular stability," *IEEE Trans. Electromagn. Compat.*, vol. 61, no. 3, pp. 878–886, 2019, DOI: 10.1109/TEMC.2018.2839881.

[33] Y. I. Abdulkarim, F. Ö. Alkurt, M. Bakir, H. N. Awl, F. F. Muhammadsharif, M. Karaaslan, B. Appasani, K. S. L. Al-Badri, Y. Zhu, and J. Dong, "A polarization-insensitive triple-band perfect metamaterial absorber incorporating ZnSe for terahertz sensing," *J. Opt.*, vol. 24, no. 10, 2022, Art. no. 105102, DOI: 10.1088/2040-8986/ac8889.

[34] M. S. U. Afsar, M. R. I. Faruque, and M. B. Hossain, "Holy cross-moon shaped dual band perfect metamaterial absorber for C-band application," *Mater. Today Commun.*, vol. 33, 2022, Art. no. 104309, DOI: 10.1016/j.mtcomm.2022.104309.

[35] M. Berka, B. Fellah, T. Islam, A. Bendaoudi, S. Das, Z. Mahdjoub, and L. Tarricone, "A triple band square-interlinked-rhombus shaped metamaterial absorber for microwave C and X-band utilizations," *Opt. Quantum Electron.*, vol. 55, no. 14, 2023, Art. no. 1223, DOI: 10.1007/s11082-023-05511-3.

[36] K. S. L. Al-Badri, "Multi band metamaterials absorber for stealth applications," *Revista de Direito, Estado e Telecomunicações*, vol. 11, no. 1, pp. 133–144, 2019, DOI: 10.26512/lstr.v11i1.22928.

[37] Y. I. Abdulkarim, L. Deng, H. Luo, S. Huang, M. Karaaslan, O. Altintas, M. Bakir, F. F. Muhammadsharif, H. N. Awl, C. Sabah, and K. S. L. Al-Badri, "Design and study of a metamaterial based sensor for the application of liquid chemicals detection," *J. Mater. Res. Technol.*, vol. 9, no. 5, pp. 10291–10304, 2020, DOI: 10.1016/j.jmrt.2020.07.034.

[38] L. Dewangan, N. K. Mishra, and S. Ghosh, "Angularly stable high-Q factor metamaterial absorber for biomedical sensing applications," *IEEE Sens. Lett.*, vol. 8, no. 8, pp. 1–4, 2024, DOI: 10.1109/LSENS.2024.3414337.

[39] M. B. Hossain, M. R. I. Faruque, M. T. Islam, M. Singh, and M. Jusoh, "Triple band microwave metamaterial absorber based on double E-shaped symmetric split ring resonators for EMI shielding and stealth applications," *J. Mater. Res. Technol.*, vol. 18, pp. 1653–1668, 2022, DOI: 10.1016/j.jmrt.2022.03.079.

[40] N. Mishra, D. K. Choudhary, R. Chowdhury, K. Kumari, and R. K. Chaudhary, "An investigation on compact ultra-thin triple band polarization independent metamaterial absorber for microwave frequency applications," *IEEE Access*, vol. 5, pp. 4370–4376, 2017, DOI: 10.1109/ACCESS.2017.2675439.

[41] S. Jorwal, A. Dubey, R. Gupta, *et al.*, "Triple-band ultrathin Minkowski fractal-inspired polarization-insensitive microwave absorber for stealth application," *J. Electron. Mater.*, vol. 53, no. 12, pp. 8171–8179, 2024, DOI: 10.1007/s11664-024-11444-8.

[42] S. Murakonda, K. S. S., and C. D. S., "Polarization-insensitive triple-band compact FSS-based absorber," *J. Electromagn. Waves Appl.*, vol. 39, no. 4, pp. 461–475, 2025, DOI: 10.1080/09205071.2025.2454394.

[43] B. Hu, S. Hong, H. Ding, *et al.*, "Dual-controlled tunable polarization-independent triple-band absorber using hybrid Dirac semimetal-vanadium dioxide metamaterial," *Opt. Quantum Electron.*, vol. 57, no. 2, 2025, Art. no. 138, DOI: 10.1007/s11082-025-08066-7.

[44] S. A. Schelkunoff, *Electromagnetic Waves*. New York, NY, USA: D. Van Nostrand, 1943.

[45] *CST Studio Suite*, Version 2022, Computer Simulation Technology, Darmstadt, Germany, 2022.